

## Composite Superabsorbent Hydrogel of Acrylic Copolymer and Eggshell: Effect of Biofiller Addition

Marcos Vinícius A. Queirós, Maslândia N. Bezerra and Judith P. A. Feitosa\*

Departamento de Química Orgânica e Inorgânica, Laboratório de Polímeros,  
Universidade Federal do Ceará, C. P. 6021, 60455-760 Fortaleza-CE, Brazil

Eggshell (ES) is an abundant waste material which is mainly composed of calcium carbonate. A superabsorbent hydrogel composite based on poly(acrylamide-*co*-potassium acrylate) as matrix containing 17 wt.% of chicken ES powder as a filler was synthesized and compared with the gel without filler. The characterization was carried out by Fourier transform infrared (FTIR), scanning electron microscopy with energy dispersive X-ray spectroscopy (SEM/EDX), thermogravimetric analysis (TGA), X-ray diffraction (XRD), rheological analysis and kinetics studies. The dispersion of ES in the polymeric matrix was homogeneous. The interaction between the acrylate and calcium cation was detected by FTIR analysis. The composite improved the gel strength and the absorption of water and saline solution increased by 100 and 41%, respectively. The high values for the swelling, the homogeneous structure and the good mechanical properties obtained with the incorporation of a relatively high content of a low-cost waste material indicate that this composite is suitable for application in the agriculture. In addition, this approach provides a more ecologically sound and useful destination for eggshell residue.

**Keywords:** polymer-matrix composite, superabsorbent hydrogel, acrylamide, acrylate, eggshell

### Introduction

Water management is in a state of crisis since there are currently more than one billion people who do not have access to safe drinking water. In addition, water resources have been shown to be insufficient to produce food in many countries. Irrigation accounts for around 70% of the total anthropogenic water use, corresponding to 2,500 out of 3,800 km<sup>3</sup>.<sup>1</sup> In arid and semi-arid regions, where water supplies are limited, agricultural practices increase the water consumption resulting in the degradation of natural ecosystems.<sup>2</sup>

In view of these problems, coupled with a growing population and a subsequent increase in food demand, the development of new technologies is necessary for the efficient use of water for agriculture. Superabsorbent polymers (SAPs), also known as hydrogels, have been used in recent years as an alternative to improve the management of water use in agricultural operations.<sup>3</sup> Hydrogels are cross-linked materials which are able to absorb and retain large amounts of water (many times their weight). They increase the water retention properties of growing media and plant growth.<sup>4</sup> SAPs are applied in soil as granules.

After watering, the granules swell and release the water slowly when the soil gets dry. The plant roots absorb water efficiently, and the loss of water through drainage or evaporation is avoided. Another advantage of SAPs is that nutritional substances can be incorporated into them and subsequently released gradually to the plants.<sup>5</sup>

Most commercial SAPs used in agriculture are pure polymers based on acrylics, normally copolymers of acrylamide and acrylate. The current trend is to add minerals to the copolymers in order to obtain a superabsorbent hydrogel composite.<sup>6,7</sup> The addition of low-cost minerals decreases the price, enhances the mechanical properties, increases water absorption and reduces the effect of salt.<sup>6-8</sup> Many researchers have studied the incorporation of waste material and clays, such as bentonite,<sup>6,8</sup> nontronite,<sup>7</sup> dolomite,<sup>8</sup> laponite<sup>9</sup> and rice husk ash,<sup>10</sup> into hydrogels.

In a study reported in the literature, hydrogel composites with dolomite provided an increase of 48% in the swelling equilibrium.<sup>8</sup> The used dolomite was composed of 73.7% (m m<sup>-1</sup>) calcium and magnesium carbonate [(CaMg(CO<sub>3</sub>)<sub>2</sub>] and 26.3% calcium carbonate (CaCO<sub>3</sub>). Carbonates seem to improve the properties of superabsorbent hydrogels based on poly(acrylamide-*co*-acrylate). Eggshell (ES) is composed mainly of calcium carbonate,

\*e-mail: judith@dqi.ufc.br

and thus its addition to hydrogels should provide an increase in water absorption.<sup>11</sup> A comparison between the effects of eggshell and dolomite on the swelling of superabsorbents can be correlated with the effects of calcium carbonate or magnesium carbonate. In addition, the use of eggshell provides an important environmental benefit, reducing the level of a waste material to be discarded by processing it into a useful product.

Eggshell (ES) is one of the most common biomaterials in nature. It is a by-product of the food industry which is normally discarded and disposed of in landfills. In 2013, the global production of eggs was almost 68 million tons.<sup>12</sup> The shell comprises around 11% of the total egg weight, and thus ca. 7.48 million tons of ES are generated as waste *per year* globally, leading to environmental problems.<sup>13,14</sup> ES is composed of 94% calcium carbonate, 1% magnesium carbonate, 1% calcium phosphate, and 4% organic materials such as sulfated polysaccharide and collagens.<sup>11</sup>

Despite being treated as a waste, many applications have been studied, mostly considering this material as a rich source of CaCO<sub>3</sub>. It has been proposed as an advanced and green alternative for a structural material in biocomposites based on epoxy formulations.<sup>15</sup> In a previous study, eggshell-derived nano- and microscale hydroxyapatite bioceramic bone grafts were synthesized.<sup>16</sup> ES has also been tested as a heterogeneous base catalyst for biodiesel production from used cooking oil.<sup>17</sup> In addition, ES has been successfully used for the removal of heavy metal ions (Ag<sup>I</sup>, Cd<sup>II</sup> and Zn<sup>II</sup>) from model solutions,<sup>18</sup> and Cr<sup>III</sup> from chrome tanning wastewater.<sup>19</sup> The co-composting of ES provides an effective liming material which can also be used for the *in situ* remediation of soils contaminated with Pb and Zn.<sup>20</sup> Due to its high thermal stability and mechanical properties, ES has been proposed as a novel biofiller for intumescent flame-retardant coatings.<sup>21</sup>

In this study, chicken eggshell powder was used as a source of calcium carbonate (CaCO<sub>3</sub>) in the synthesis of a superabsorbent hydrogel composite from poly(acrylamide-*co*-potassium acrylate). The effect of the addition of eggshell to the copolymer was evaluated by comparing the swelling kinetics of the copolymer (Pam-Ac) and the composite (Pam-Ac/ES) in distilled water. The behavior of the hydrogels was also investigated in salt solution.

## Experimental

### Reagents

Acrylamide (Am), potassium persulfate (KPS) and *N,N,N',N'*-tetramethylethylenediamine (TEMED) were obtained from Merck. *N,N'*-Methylenebisacrylamide

(MBA) was purchased from Sigma-Aldrich and acrylic acid (AA) from Vetec. The degree of purity for both Am and AA was higher than 99%. The acrylic acid was neutralized with KOH until pH 7.0 in an ice bath to prepare potassium acrylate (KAc). White chicken eggs were obtained from a local store. The shells were washed, sanitized with NaClO solution, oven-dried, grated using a stainless steel sieve (Bertel Indústria Metalúrgica Ltda) and separated into three different size fractions. The fraction with a particle size of smaller than 45 µm (325 mesh sieve) was employed in this study. Distilled water was used in all of the experiments.

### Synthesis of hydrogels

The hydrogels were synthesized by free-radical copolymerization following the procedure reported by Magalhães *et al.*<sup>22</sup> with a few modifications. Acrylamide (1.05 g, 0.015 mol, in 1 mL) was added to 24 mL of distilled water constantly bubbled with nitrogen. After dissolution, obtained with stirring, aqueous KAc (3 mL, 5 mol L<sup>-1</sup>, 0.015 mol) was added. MBA (0.2 mol% in 1 mL related to the total number of mols of monomers), KPS (0.2 mol% in 1 mL) and TEMED (0.1 mol%) were then also added. The total volume was maintained at 30 mL. The system was kept under further stirring until it reached the gel point. After 24 h, the hydrogel was grated, washed and dried in an oven at 70 °C. The material was sieved in order to obtain samples with particle sizes in the range of 500 to 710 µm (24-35 mesh). The obtained hydrogel was named Pam-Ac.

The appropriate amount of eggshell in the hydrogel was defined after an initial screening in which the content of the additive was varied from 9 to 33% (wt.%), with increments of 4%. The degree of swelling in water was determined and the highest value was obtained for the hydrogel containing 17% of eggshell. Thus, this percentage of ES was employed in the study. The hydrogel with eggshell powder (named Pam-Ac/ES) was synthesized applying the procedure described above for the hydrogel without filler, with some modifications. An aqueous suspension (24 mL) of eggshell powder (0.534 g) was stirred for 24 h in order to disaggregate the material. The co-monomers were added to this suspension and the above-described procedure was followed. The total volume was maintained at 30 mL. The particle size was the same as that of the hydrogel without addition of minerals (500-710 µm).

### Elemental microanalysis

The contents of carbon, hydrogen and nitrogen were obtained by elemental microanalysis using a Carlo Erba EA 1108 analyzer.

### X-ray diffraction (XRD) analysis

The XRD analysis of the eggshell powder was carried out on a PANalytical diffractometer (model XPert Pro MPD), with Cu K $\alpha$  radiation, with  $2\theta$  varying from  $10^\circ$  to  $70^\circ$ . The material was sieved and only the particles that passed through a 325 mesh ( $< 45 \mu\text{m}$ ) were selected for analysis.

### Infrared spectroscopy studies

The Fourier transform infrared (FTIR) spectra for dried samples of Pam-Ac and Pam-Ac/ES were recorded with a Shimadzu IR spectrophotometer (model FT IR-8500) in the range of 400 to 4000  $\text{cm}^{-1}$  using KBr pellets.

### Thermogravimetric analysis (TGA)

The thermal degradation behavior was monitored using a TA Instruments thermogravimetric analyzer (model TGA-Q50). The samples (2.5-3.5 mg) were placed in a platinum pan and heated to 1000  $^\circ\text{C}$  using a 10  $^\circ\text{C min}^{-1}$  heating ramp in a synthetic air environment with an air flow of 50  $\text{cm}^3 \text{min}^{-1}$ . The particles which passed through a 45 mesh sieve were subject to analysis.

### Scanning electron microscopy (SEM)

Surface images of the eggshell and hydrogels were obtained on an Inspect S50 scanning electron microscope coupled to an energy dispersive X-ray spectrometer (SEM-EDX). Small slices of samples, swollen in distilled water until equilibrium, were frozen with liquid nitrogen, dried by freeze-drying and coated with gold prior to the analysis.

### Rheology: dynamic tests

Rheological measurements were performed using a TA Instruments rheometer (model AR550) with parallel plate geometry and with a plate diameter of 20 mm at 25  $^\circ\text{C}$ . The measurements were taken using the previously synthesized hydrogels. To obtain the materials, synthesis was carried out following the method described above, but a test-tube was used instead of a reactor to obtain cylindrical gels with the same diameter (20 mm). After synthesis, the hydrogels were left to stand for 24 h. The test-tube was then broken and the gel was cut into cylindrical shapes with a height of 0.5 cm. The oscillatory measurements were carried out at a frequency range of 0.1-1.5 Hz.

### Degree of swelling in distilled water

The swelling kinetics of Pam-Ac and Pam-Ac/ES in distilled water at  $25 \pm 1 \text{ }^\circ\text{C}$  were compared. A known mass of gel (approximately 20 mg) was placed inside a pre-weighed sintered glass-filter (No. 0) and covered with distilled water at room temperature. The glass filter was then removed and the excess water was drained. The external walls were dried and the system was re-weighed. Initially, the systems were weighed at intervals of 1.0 min, and then at longer intervals. The degree of swelling was determined according to equation 1:

$$W_{\text{eq}} = (m_{\text{sw}} - m_{\text{dr}}) / m_{\text{dr}} \quad (1)$$

where  $W_{\text{eq}}$  is the equilibrium degree of swelling,  $m_{\text{sw}}$  is the mass of swollen material and  $m_{\text{dr}}$  is the mass of the dried material.

### Swelling in salt solution

The behavior of the hydrogels in a solution designed to simulate soil conditions was also investigated at  $25 \pm 1 \text{ }^\circ\text{C}$ . The materials were immersed in a salt solution with a composition of NaCl (0.2  $\text{mmol L}^{-1}$ ), KCl (0.2  $\text{mmol L}^{-1}$ ),  $\text{MgCl}_2$  (0.2  $\text{mmol L}^{-1}$ ) and  $\text{CaCl}_2$  (0.3  $\text{mmol L}^{-1}$ )<sup>23-25</sup> and the swelling was determined as described above.

## Results and Discussion

### Characterization of the chicken eggshell powder

The diffraction pattern for the eggshell powder shown in Figure 1 was compared with the calcite pattern calculated from ICSD data using POWD-12++. The most intense peak at a  $2\theta$  value of  $29.5^\circ$  corresponds to the {104} plane of calcite.<sup>15</sup> The two powder diffraction patterns show good agreement. The chemical composition of the eggshell obtained by XRF showed a large amount of calcium ( $99.09 \pm 0.29\%$ ) followed by very low amounts of phosphorous ( $0.26 \pm 0.04\%$ ), probably present as calcium phosphate and sulfur ( $0.28 \pm 0.04\%$ ) associated with sulfated polysaccharides.<sup>14</sup>

The TGA and differential thermogravimetry (DTG) curves for the eggshell are shown in Figure 2. A very small decrease in mass can be observed between 226 and 574  $^\circ\text{C}$  due to the decomposition of residual organic matter. The main event takes place within the temperature range of 574-731  $^\circ\text{C}$  and is attributed to thermal decomposition of  $\text{CaCO}_3$  with the release of  $\text{CO}_2$ . The residue at 800  $^\circ\text{C}$  (52.8%) refers to inorganic compounds, in this case  $\text{CaO}$ .<sup>26</sup>

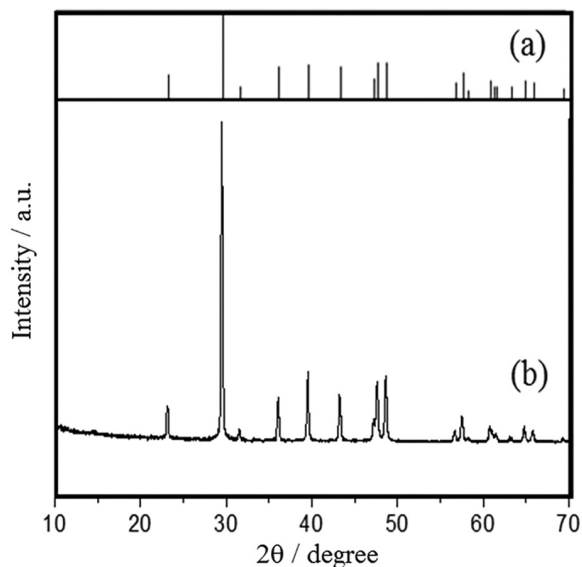


**Figure 1.** X-ray profiles for (a) calcite and (b) eggshell (reference code 85-1108).

This value is close to that of the residue of pure  $\text{CaCO}_3$  shown in the figure (55.9%). The  $\text{CaCO}_3$  content was determined through the loss of  $\text{CO}_2$  in the third stage by stoichiometric calculations, giving a value of 94.4%, which is in agreement with the value of 94% reported in the literature.<sup>14</sup>

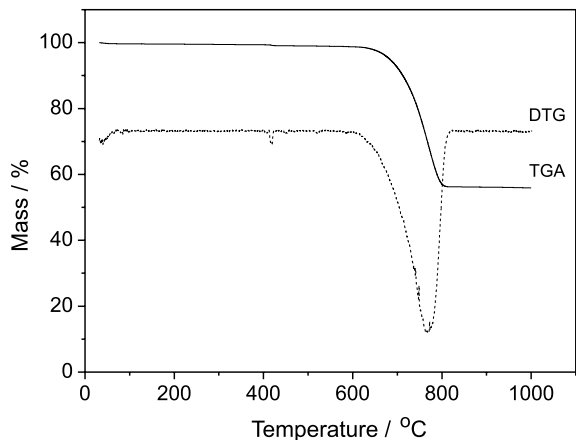


**Figure 2.** TGA/DTG curves for eggshell powder.

### Characterization of hydrogels

#### Infrared spectroscopy studies

The FTIR spectra for Pam-Ac, ES and the Pam-Ac/ES composite can be observed in Figure 3, and the assignments are shown in Table 1. Peaks due to the carbonate vibration modes are present at  $1421\text{ cm}^{-1}$  ( $\nu_3$ ),  $876\text{ cm}^{-1}$  ( $\nu_2$ ) and  $713\text{ cm}^{-1}$  ( $\nu_4$ ), as indicated on the eggshell spectrum. A shoulder appears at  $1084\text{ cm}^{-1}$  ( $\nu_1$ ), which is attributed to the symmetric stretching of  $\text{CO}_3^{2-}$ .<sup>28</sup> Two other bands are related to combination bands, that is  $\nu_1 + \nu_4$  at  $1801\text{ cm}^{-1}$  and

$\nu_1 + \nu_3$  at  $2518\text{ cm}^{-1}$ . Bands associated with adsorbed water were also observed at  $3380$  and  $1643\text{ cm}^{-1}$ . The presence of organic material can be deduced from the appearance of a band in the region of  $2924$ - $2867\text{ cm}^{-1}$ . In the Pam-Ac spectrum, the important bands are those at  $1675\text{ cm}^{-1}$  ( $\text{C}=\text{O}$  from acrylamide),  $1568\text{ cm}^{-1}$  ( $\nu_{\text{as}}\text{COO}^-$  from acrylate) and  $1399\text{ cm}^{-1}$  ( $\nu_{\text{s}}\text{COO}^-$  from acrylate). Similar bands can be observed on the Pam-Ac/ES spectrum. The difference between  $\nu_{\text{as}}\text{COO}^-$  and  $\nu_{\text{s}}\text{COO}^-$  could be related to the metal-carboxylate interaction.<sup>29</sup> A comparison was made between free  $\Delta\nu(\text{COO}^-)$  and  $\Delta\nu(\text{COO}^-)$  bound to di- or trivalent cations. The carboxylate of the copolymer interacts with the  $\text{Ca}^{2+}$  of the eggshell calcite. The values obtained for  $\Delta\nu$  were  $\Delta\nu(\text{COO}^-)_{\text{K}}$  in Pam-Ac  $170\text{ cm}^{-1}$  and  $\Delta\nu(\text{COO}^-)_{\text{Ca}}$  in Pam-Ac/ES  $147\text{ cm}^{-1}$ . The decrease in  $\Delta\nu$  indicates the coordination of metal cations to the carboxylate, which verifies the calcite-acrylate interaction. A similar trend was observed for  $\text{Ca}^{2+}$ -alginate, in which the difference in  $\Delta\nu$  was  $13\text{ cm}^{-1}$ .<sup>29</sup> This difference was higher for Pam-Ac/ES ( $23\text{ cm}^{-1}$ ), confirming the  $\text{Ca}^{2+}$ - $\text{COO}^-$  or eggshell powder-copolymer interaction.

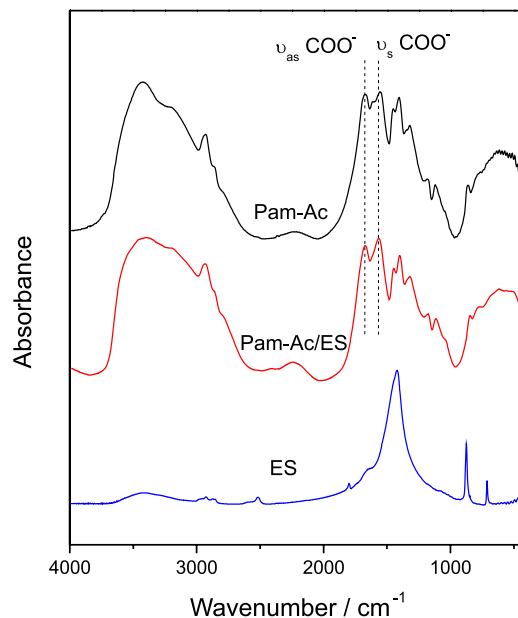


**Figure 3.** FTIR spectra for eggshell powder (ES) and hydrogels.

#### Elemental microanalysis

The results for the chemical analysis of Pam-Ac and Pam-Ac/ES are given in Table 2. Considering that all of the nitrogen content originates from the acrylamide monomeric unit  $[-\text{CH}(\text{CONH}_2)\text{CH}_2-]$ , the mols of Am in 100 g of hydrogel (%mol Am) can be calculated. Acrylamide and K acrylate  $[-\text{CH}(\text{COOK})\text{CH}_2-]$  contain carbon. On determining the carbon associated with acrylamide, the mols of acrylate in 100 g of hydrogel (%mol KAc) can be

**Table 1.** Assignments of the main bands of the FTIR spectra for eggshell (ES), and for hydrogels Pam-Ac and Pam-Ac/ES

ES	Hydrogel		Assignment <sup>22,27,28</sup>
	Pam-Ac	Pam-Ac/ES	
–	3427	3413	$\nu_{as}NH_2$ of acrylamide unit
3380	3219	3219	$\nu OH$ of adsorbed water
–	3195	–	$\nu_sNH_2$ of acrylamide unit
2924-2867	2933 and 2860	2933 and 2857	$\nu CH$ and $\nu CH_2$
2516	–	–	combination band $CO_3^-$
1799	–	–	combination band $CO_3^-$
–	1670	1670	$\nu C=O$ of acrylamide
1657	–	–	$\delta OH$ of water
–	1569	1554	$\nu_{as}COO^-$ of K-acrylate
1421	–	–	$\nu_{as}CO_3^-$
–	1399	1407	$\nu_sCOO^-$ of K-acrylate and $\nu CN$ of acrylamide
878	–	–	$\delta_{out\ plane}CO_3^-$
713	–	–	$\delta_{in\ plane}CO_3^-$

calculated. The equations used to determine the molar ratio of Am/KAc in the Pam-Ac hydrogels were

$$\%mol\ Am = \frac{\%N}{14} \quad (2)$$

$$\%mol\ C\ from\ KAc = \frac{\%C}{12} - \frac{3\%N}{14} \quad (3)$$

$$\%mol\ KAc = \frac{\%mol\ C\ from\ KAc}{3} = \left( \frac{\%C}{12} - \frac{3\%N}{14} \right) / 3 \quad (4)$$

$$\text{molar ratio of } \frac{Am}{KAc} = \frac{\frac{3\%N}{14}}{\frac{\%C}{12} - \frac{3\%N}{14}} \quad (5)$$

In the case of Pam-Ac/ES, the carbon content associated with carbonate can be determined using equation 3. The percentage (by weight) of eggshell in the hydrogel was 16.7 and the calcium carbonate content in ES was determined as 94.4%. Thus, the calcium carbonate content in 100 g of hydrogel was 15.8%. The molar mass of  $CaCO_3$  is  $100\ g\ mol^{-1}$ . Therefore

$$\begin{aligned} \%mol\ C\ from\ ES\ carbonate = \\ \%mol\ of\ Ca\ carbonate\ in\ hydrogel = \frac{15.8}{100} \end{aligned} \quad (6)$$

$$\%mol\ C\ from\ KAc = \frac{\%C}{12} - \frac{3\%N}{14} - 0.17 \quad (7)$$

$$\text{molar ratio of Am/KAc} = \frac{\frac{3\%N}{14}}{\frac{\%C}{12} - \frac{3\%N}{14} - 0.158} \quad (8)$$

For Pam-Ac, this value was  $1.05 \pm 0.18$ , very close to the theoretical value (1.00). The Am/KAc value for Pam-Ac/ES was  $1.28 \pm 0.05$ . Similar results were obtained for Pam-KAc in the absence ( $Am/Kac = 0.96$ ) and in the presence ( $Am/Kac = 1.2$ ) of 10% of dolomite.<sup>8</sup> The higher value in the composite hydrogels is probably related to the lower availability of acrylate due to its complexation with  $Ca^{2+}$  and/or other positively-charged functional groups at the calcite surface.<sup>30</sup>

#### Thermogravimetric analysis (TGA)

The thermal decomposition curve for Pam-Ac is shown in Figure 4. Four stages can be observed: the first two stages (323 and 391 °C) being attributed to the decomposition of acrylamide units and the other stages to the decomposition of acrylate units (550 and 883 °C). At 1000 °C, the final residue is zero. According to Dassanayake and Phillips,<sup>31</sup> the thermal decomposition of polyacrylamide occurs at 492 °C and the thermal decomposition of polyacrylate starts at higher temperatures. In addition, Silva *et al.*<sup>32</sup> reported that the thermal degradation of dry polyacrylamide occurs in two stages (at 326 and 410 °C). The experimental TGA curve in Figure 4 is similar to those reported by the above cited authors. The Am/KAc mass ratio was calculated from the mass loss of each monomer, giving a value of 1.09. In the TGA curve for Pam-Ac/ES (Figure 4), there is another

**Table 2.** Elementary chemical composition of hydrogels Pam-Ac and Pam-Ac/ES obtained from microanalysis

Hydrogel	Composition / wt. %			Am/Ac ratio
	C	H	N	
Pam-Ac	31.94 ± 2.53	5.54 ± 0.04	6.40 ± 1.01	1.05 ± 0.18
Pam-Ac/ES	31.94 ± 0.11	5.46 ± 0.04	6.56 ± 0.13	1.28 ± 0.05

stage at 550-675 °C related to the decomposition of the eggshell. As previously described, a high rate of mass loss occurs due to the release of CO<sub>2</sub> from CaCO<sub>3</sub>. At this stage, the real content of mineral in the hydrogel was calculated and the value obtained was 17.2 wt.%, which is close to the expected value (16.5 wt.% to Pam-Ac/ES).

#### SEM-EDX analysis

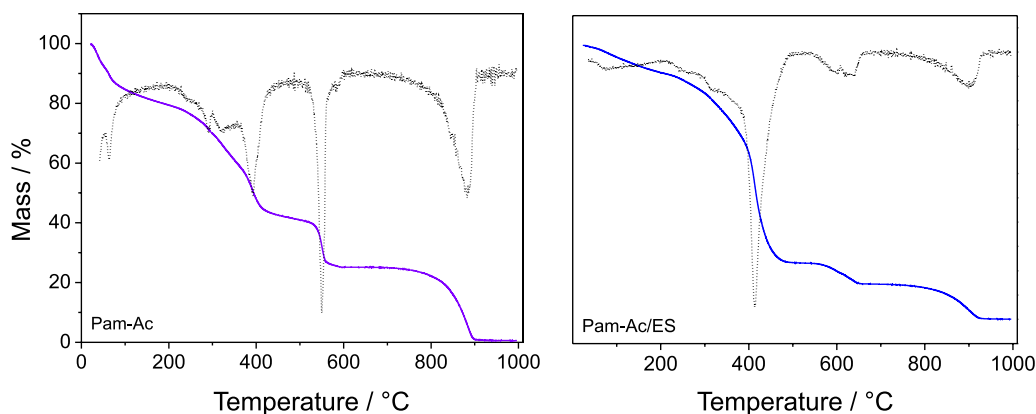
The SEM analysis of Pam-Ac showed a fibrous surface with pores (Figure 5a). The morphology of the Pam-Ac/ES surface (Figure 5b) differed from that of the Pam-Ac surface. Pore diameters are smaller and the surface more irregular. Interestingly, crystals with the dimensions of those of ES (3-9 μm) were not observed in the composite hydrogel. Thus, it appears that the crystals were well dispersed during the synthesis. The acrylate monomer is well distributed along the surface of the hydrogel, as shown by the K-EDX results. A similar distribution can be observed on the Ca-EDX micrograph.

Rheological experiments were conducted to obtain the linear viscoelastic region in the range of 0-10 Pa at a fixed frequency of 0.1 and 1.5 Hz. A constant stress of 5.0 Pa was selected to conduct the frequency sweep. The rheological results are given in Figure 6. The storage modulus ( $G'$ ) values for the Pam-Ac and Pam-Ac/ES hydrogels decreased as the frequency increased. This is due to the fact that the time available was not sufficient for chain disentanglement and relaxation.<sup>33</sup> The addition of eggshell increased the storage modulus of the Pam-Ac hydrogel. Higher gel strength resulted from the presence of the filler. The loss

modulus ( $G''$ ) remains almost constant with variations in the frequency and is much lower than the  $G'$  values for the two hydrogels. The  $\tan \delta$  value calculated from the  $G''/G'$  ratio (data not shown) was smaller than 1.0 across the whole frequency range. This indicates an elastic nature or a typical solid-like behavior for both hydrogels.

#### Swelling kinetics

The swelling kinetics of Pam-Ac and Pam-Ac/ES can be seen in Figure 7a for water and for the salt solution. In all cases, the swelling rate is higher during the first few minutes and then reaches an equilibrium plateau. A higher degree of swelling was presented by Pam-Ac/ES, in the case of water reaching  $1256 \pm 39$  g water g<sup>-1</sup> dry hydrogel. On adding mineral loads to a polymer there is an increase in the hydrophilicity, which leads to a greater difference in the osmotic pressures of the gel and external solution. In the case of water, the degree of swelling for Pam-Ac/ES was around twice that for Pam-Ac ( $629 \pm 28$  g water g<sup>-1</sup> dry hydrogel for the latter). The degree of swelling in water obtained for Pam-Ac/ES in this study is higher than results previously reported for gels containing different minerals, such as bentonite 34%,<sup>6</sup> dolomite 52%,<sup>8</sup> sepiolite 14-60%<sup>34</sup> and nontronite 71%.<sup>7</sup> The maximum content of mineral in these cited gels was 10 wt.%. Taking into account the higher content of filler and the fact that eggshell is currently treated as a waste material, the water absorbance capacity of Pam-Ac/ES reported herein is an excellent result.

**Figure 4.** TGA/DTG curves for hydrogels.

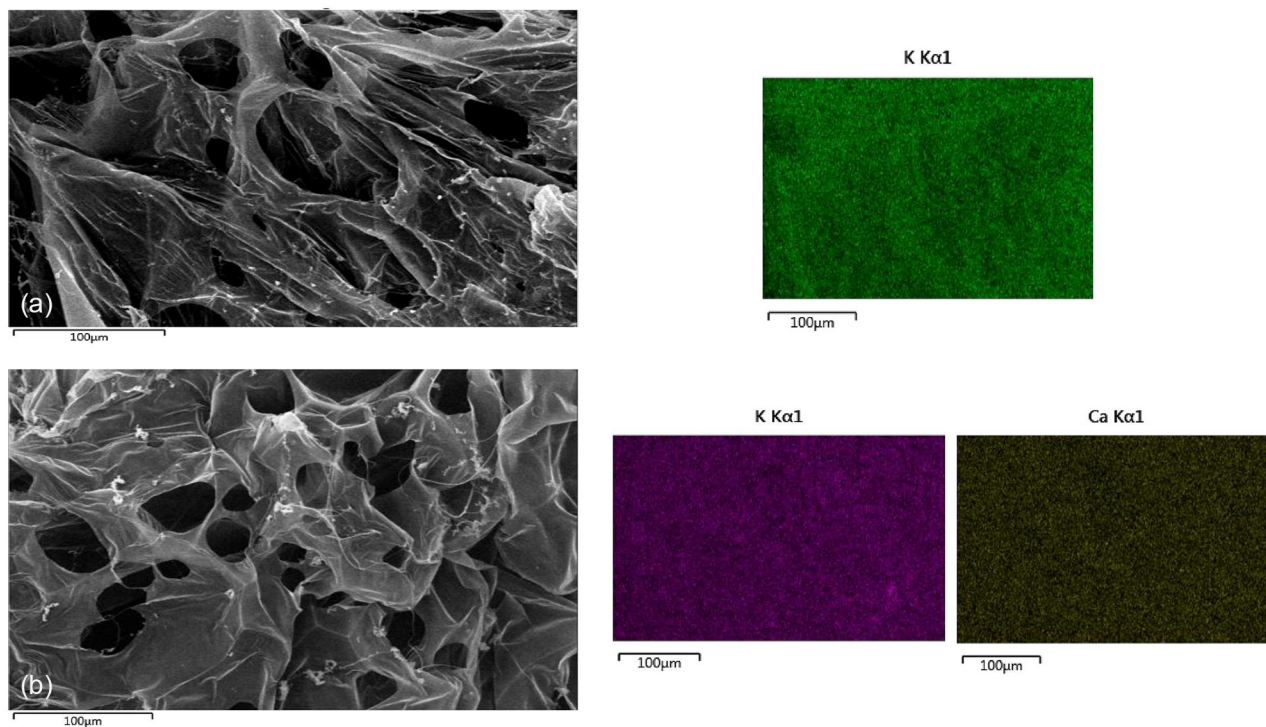


Figure 5. SEM and EDX images for hydrogels (a) Pam-Ac and (b) Pam-Ac/ES.

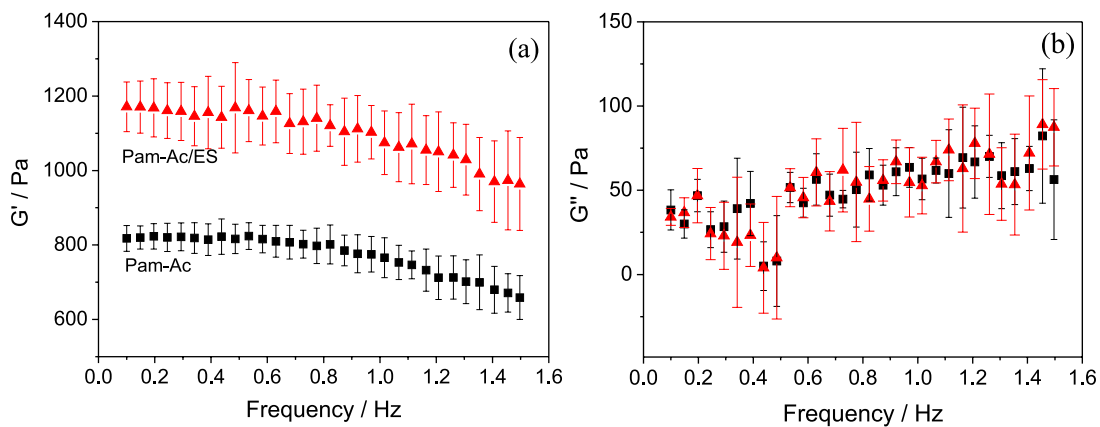


Figure 6. (a) Storage modulus ( $G'$ ) and (b) loss modulus ( $G''$ ) for hydrogels (■) Pam-Ac and (▲) Pam-Ac/ES.

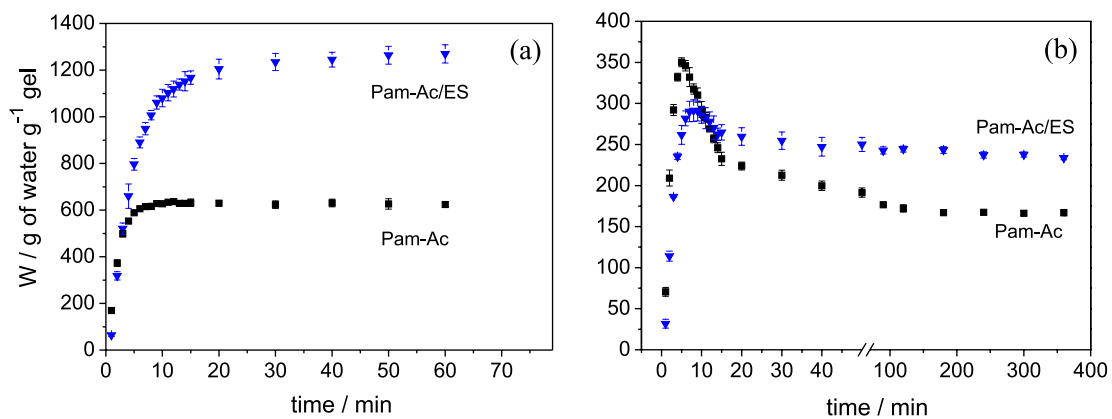


Figure 7. Swelling kinetics plot obtained for hydrogels in (a) distilled water and (b) salt solution.

An important parameter is the rate constant of swelling. In general, the swelling follows a first-order or a second-order kinetics.<sup>35</sup> The second-order rates may be obtained from the well-known equation

$$t/W = [1/kW_{eq}^2] + [1/W_{eq}]t \quad (9)$$

where  $W$  is the swelling degree at time  $t$ ,  $W_{eq}$  is the equilibrium swelling degree and  $k$  is a second-order rate constant.

The plot of  $t/W$  vs.  $t$  is given in Figure 8. It can be observed that almost all of the experimental points lie on the respective straight lines for each hydrogel. However, the values did not fit the straight lines in the first few minutes, suggesting a different kinetics order, probably a first-order process, as suggested by Diez-Peña *et al.*<sup>35</sup> A new plot (not shown) was obtained without the initial points and a better fit and linear correlation coefficients ( $R^2$ ) were observed. The  $R^2$  value for the straight line for Pam-Ac increases from 0.9992 to 0.9995. However, the improvement in  $R^2$  is much better for the Pam-Ac/ES hydrogel (0.9738 to 0.9999). Two parameters,  $W_{eq}$  and  $k$ , were calculated from the slope ( $1/W_{eq}$ ) and intercept ( $1/kW_{eq}^2$ ) of the lines and the results are shown in Table 3. The second-order rate constant for Pam-Ac is higher than that for Pam-Ac/ES.

The initial rate constants  $k_i$  were determined from plots of  $\ln[1 - W/W_{eq}]$  vs.  $t$  as the slope of the straight lines ( $-k_i$ ) for the swelling of the hydrogels in water. The initial rate

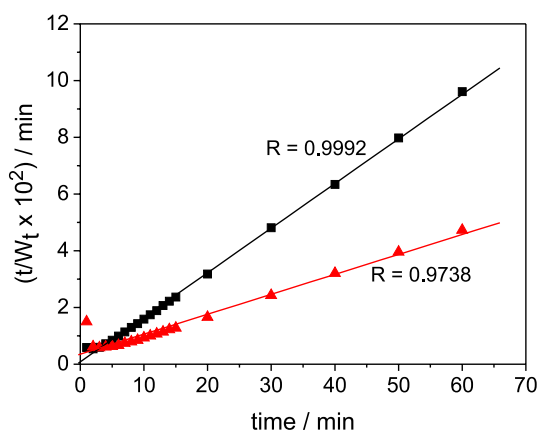


**Figure 8.** Second-order kinetics plot for swelling of hydrogels: (■) Pam-Ac and (▲) Pam-Ac/ES.

**Table 3.** Kinetics parameters in distilled water and salt solution simulating soil conditions (SSS)

Hydrogel	First-order kinetics in water <sup>a</sup>		Second-order kinetics in water <sup>b</sup>		
	$k_i / \text{min}^{-1}$	$R^2$	$k / (\text{L mol min}^{-1})$	$W_{eq} / (\text{g water g}^{-1} \text{ dry gel})$	$R^2$
Pam-Ac	0.609	0.9992	$5.51 \times 10^{-3}$	631	0.9995
Pam-Ac/ES	0.236	0.9995	$3.66 \times 10^{-4}$	1314	0.9999

<sup>a</sup>For the first 5 min; <sup>b</sup>without the first points;  $R^2$ : linear correlation coefficient.

constants are higher than the second-order rate constants for both hydrogels. The Pam-Ac hydrogel gave the highest rate constant. The experimental data were plotted according to the first-order equation:<sup>35</sup>

$$W/W_{eq} = 1 - e^{-kt} \quad (10)$$

The swelling degree of the hydrogels was also evaluated in a salt solution aimed at simulating the conditions in soil. The profiles of the swelling curves obtained in salt solution (Figure 7b) differed from those obtained in distilled water. There was a fast absorption of water in the first few minutes followed by mass loss until reaching equilibrium. The curves can be divided into four stages. In the first, the hydrogel swells due to the uptake of water. This is the fastest swelling stage, characterized by an increasing swelling rate. In the second stage, divalent ions are absorbed along with water and the swelling reaches the highest value. In the third stage, there is an exchange between the monovalent ions ( $\text{Na}^+$  and  $\text{K}^+$ ) in the polymeric network and divalent ions in the solution, which coordinate with the carboxylate group in the hydrogel.<sup>36</sup> In the last stage, the swelling decreases until equilibrium. The swelling of Pam-Ac/ES in the salt solution simulating soil conditions was 41% higher in comparison with the hydrogel without filler, this performance being better than that previously observed for Pam-Ac/Dol (34% increase in swelling).<sup>8</sup>

## Conclusions

The incorporation of 17 wt.% of eggshell waste powder into poly(acrylamide-*co*-potassium acrylate) improves the absorption of the hydrogel by 100 and 41% for water and saline solution, respectively, in comparison with the gel without the addition of the waste material. A gel that absorbs an amount of water representing more than 1,000 times its own dry weight was obtained. The dispersion of ES in the polymeric matrix is homogeneous. Interaction between the acrylate in the gel and calcium cation in the eggshell was verified. The composite hydrogel provides a stronger material with a high degree of swelling in water and in salt solution, a homogeneous structure and good mechanical properties. These important advantages, plus the relatively high content

of a low-cost material which would otherwise be treated as a waste material, make Pam-Ac/ES suitable for application in agriculture. In addition, it offers an ecologically sound and widely applicable destination for eggshell residue.

## Acknowledgments

The authors acknowledge financial support from the Brazilian governmental agencies INCT-INOMAT, Conselho Nacional de Desenvolvimento Científico e Tecnológico (CNPq), and Coordenação de Aperfeiçoamento de Pessoal de Nível Superior (CAPES). We are also grateful to Central Analítica (UFC).

## References

1. Cosgrove, W. J.; Rijsberman, R.; *World Water Vision*; Earthscan Publications: London, UK, 2000.
2. Hochmuth, H.; Thevs, N.; He, P.; *Environ. Earth Sci.* **2015**, *73*, 5269.
3. Chandrika, K. S. V. P.; Singh, A.; Sarkar, D. J.; Rathore, A.; Kumar, A.; *J. Appl. Polym. Sci.* **2014**, *41060*, 1.
4. Montesano, F. F.; Parente, A.; Santamaria, P.; Sannino, A.; Serio, F.; *Agr. Agr. Sci. Procedia* **2015**, *4*, 451.
5. Cannazza, G.; Cataldo, A.; De Benedetto, E.; Demitri, C.; Madaghiele, M.; Sannino, A.; *Water* **2014**, *6*, 2056.
6. Kalaleh, H.-A.; Tally, M.; Atassi, Y.; *Polym. Sci., Ser. B* **2015**, *57*, 750.
7. Leitão, R. C. F.; de Moura, C. P.; da Silva, L. R. D.; Ricardo, N. M. P. S.; Feitosa, J. P. A.; Muniz, E. C.; Fajardo, A. R.; Rodrigues, F. H. A.; *Quim. Nova* **2015**, *38*, 370.
8. Magalhães, A. S. G.; Almeida Neto, M. P.; Bezerra, M. N.; Feitosa, J. P. A.; *J. Braz. Chem. Soc.* **2013**, *24*, 304.
9. Li, P.; Kim, N. H.; Siddaramaiah, J. H. L.; *Composites, Part B* **2009**, *40*, 275.
10. Cândido, J. S.; Pereira, A. G. B.; Fajardo, A. R.; Ricardo, N. M. P. S.; Feitosa, J. P. A.; Muniz, E. C.; Rodrigues, F. H. A.; *Composites, Part B* **2013**, *51*, 24653.
11. Li, Y.; Xin, S.; Bian, Y.; Xu, K.; Han, C.; Dong, L.; *Int. J. Biol. Macromol.* **2016**, *85*, 63.
12. Food and Agriculture Organization of the United Nations (FAO); <http://www.fao.org/faostat/en/#compare>, accessed on March 6, 2017.
13. Oliveira, D. A.; Benelli, P.; Amante, E. R.; *J. Cleaner Prod.* **2013**, *46*, 42.
14. Rossi, M.; Nys, Y.; Anton, M.; Bain, M.; De Ketelaere, B.; de Reu, K.; Dunn, I.; Gautron, J.; Hammershøj, M.; Hidalgo, A.; Meluzzi, A.; Mertens, K.; Nau, F.; Sirri, F.; *World's Poultry Sci. J.* **2013**, *69*, 414.
15. Tiimob, B. J.; Jeelani, S.; Rangari, V. K.; *J. Appl. Polym. Sci.* **2016**, *133*, 43124.
16. Demirel, M.; Aksakal, B.; *J. Sol-Gel Sci. Technol.* **2016**, *78*, 126.
17. Tan, Y. H.; Abdullah, M. O.; Hipolito, C. N.; Yap, Y. H. T.; *Appl. Energy* **2015**, *160*, 58.
18. Baláž, M.; Ficeriová, J.; Briančin, J.; *Chemosphere* **2016**, *146*, 458.
19. Elabbas, S.; Mandi, L.; Berrekhis, F.; Pons, M. N.; Leclerc, J. P.; Ouazzani, N.; *J. Environ. Manage.* **2016**, *166*, 589.
20. Soares, M. A. R.; Quina, M. J.; Ferreira, R. M. Q.; *J. Environ. Manage.* **2015**, *164*, 137.
21. Yew, M. C.; Ramli Sulong, N. H.; Yew, M. K.; Amalina, M. A.; Johan, M. R.; *Prog. Org. Coat.* **2015**, *81*, 116.
22. Magalhães, A. S. G.; Almeida Neto, M. P.; Bezerra, M. N.; Ricardo, N. M. P. S.; Feitosa, J. P. A.; *Quim. Nova* **2012**, *35*, 1464.
23. Lindroos, A.-J.; Brügger, T.; Derome, J.; Derome, K.; *Water, Air, Soil Pollut.* **2003**, *149*, 269.
24. Ludwig, B.; Khanna, P. K.; Raison, R. J.; Jacobsen, K. L.; *Forest Ecol. Manage.* **1998**, *103*, 9.
25. Hammecker, C.; van Asten, P.; Marlet, S.; Maeght, J.-L.; Poss, R.; *Geoderma* **2009**, *150*, 129.
26. Khemthong, P.; Luadthong, C.; Nualpaeng, W.; Changsuwan, P.; Tongprem, P.; Viriya-Empikul, N.; Faungnawakij, K.; *Catal. Today* **2012**, *190*, 112.
27. Xu, B.; Toffolo, M. B.; Regev, L.; Boaretto, E.; Poduska, K. M.; *Anal. Methods* **2015**, *7*, 9304.
28. Al-Hosney, H. A.; Grassian, V. H.; *Phys. Chem. Chem. Phys.* **2005**, *7*, 1266.
29. Papageorgiou, S. K.; Kouvelos, E. P.; Favvas, E. P.; Sapolidis, A. A.; Romanos, G. E.; Katsaros, F. K.; *Carbohydr. Res.* **2010**, *345*, 469.
30. Li, S.; Leroy, P.; Heberling, F.; Devau, N.; Jougnot, D.; Chiaberge C.; *J. Colloid Interface Sci.* **2016**, *468*, 262.
31. Dassanayake, N. L.; Phillips, R. W.; *Anal. Chem.* **1984**, *56*, 1753.
32. Silva, M. E. S. R.; Dutra, E. R.; Mano, V.; Machado, J. C.; *Polym. Degrad. Stab.* **2000**, *67*, 491.
33. Ramazani-Harandi, M. J.; Zohuriaan-Mehr, M. J.; Yousefi, A. A.; Ershad-Langroudi, A.; Kabiri, K.; *J. Appl. Polym. Sci.* **2009**, *113*, 3676.
34. Santiago, F.; Mucientes, A. E.; Osorio, M.; Poblete, F. J.; *Polym. Int.* **2006**, *55*, 843.
35. Diez-Peña, E.; Quijada-Garrido, I.; Barrales-Rienda, J. M.; *Macromolecules* **2002**, *35*, 8882.
36. Zheng, Y.; Li, P.; Zhang, J.; Wang, A.; *Eur. Polym. J.* **2007**, *43*, 1691.

Submitted: October 17, 2016

Published online: March 9, 2017